Boron-doped diamond synthesized by chemical vapor deposition as a heating element in a multi-anvil apparatus

Longjian Xie[1*], Akira Yoneda[2], Zhaodong Liu[1], Nishida Keisuke[1], Tomoo Katsura[1]

1. *Bayerisches Geoinstitut, University of Bayreuth, Bayreuth 95440, Germany*
2. *Institute for Planetary Materials, Okayama University, Misasa, Tottori 682-0193, Japan*

[*]Corresponding author. Tel: +49 (0)921 55 3743; Fax: +49 (0)921 55 3769.

E-mail: Longjian.Xie@uni-bayreuth.de

Accepted manuscript

https://doi.org/10.1080/08957959.2020.1789618

Abstract:

We tested boron doped diamond (BDD) synthesized by chemical vapor deposition (CVD) as a heating element in a multi-anvil apparatus. We succeeded in manufacturing BDD into a tubular shape by laser cutting and electric discharging machining. The BDD tube shaped by the electric discharging machining was contaminated by discharging electrode materials (Mo and W), which affected the heating performance. The laser-cut BDD tube has a clean surface, and therefore had a good heating performance. We succeeded in generating temperature as high as 2670 K at a pressure around 30 GPa with laser-cut heater. Heating reproducibility was confirmed through repeated heating and cooling cycles. The recovered sample shows that a higher temperature generation above 2670 K was prevented by eutectic melting of ZrO_2 thermal insulator and Al_2O_3 sample. Owing to the commercial availability with a reasonable price, CVD-BDD heaters are more practical than a high-pressure synthesized BDD heaters for wide applications.

Key words: Chemical vapor deposition, Boron-doped diamond, Multi-anvil apparatus, High temperature generation, X-ray transparency

I. Introduction

Multi-anvil apparatus (MAA) has a capability to generate lower mantle pressures (>23 GPa), and is an important tool to study physical and chemical properties of deep-Earth materials [1]. Temperatures over 3000 K are vital for melting of mantle materials under lower-mantle conditions [e.g. 2-5]. Because of the refractory and X-ray transparency, boron-doped diamond (BDD) is a good heating material for ultrahigh-temperature generation using electrical resistive heating in MAA [6] and diamond anvil cell [7]. It has recently drawn a special attention after its successful temperature generation up to 4000 K [6] and application to viscosity measurement of silicate melts at pressures to 30 GPa and temperatures to 3300 K in MAA [8].

In these studies, significant efforts have been made to find the best form of BDD (precursor or pre-synthesized BDD) for manufacturing furnaces [6, 9-12]. The stable temperature generation up to 4000 K demonstrated overall advantage of pre-synthesis than in-situ synthesis using a graphite-boron composite as a precursor [6]. In those studies, BDD tubes were directly synthesized at high pressure or molded from powders, which was ground from high-pressure synthesized BDD blocks [6,8]. These tremendous efforts and costs for preparation limited its wide variety of applications. A convenient way to obtain BDD is thus needed. Moreover, the assembly size dramatically decreases to generate higher pressures. For experiments above 30 GPa, the edge lengths of octahedral pressure media are less than 7 mm in the majority of studies, and small heaters accommodated in such small volumes should have thin walls with thickness less than 0.2 mm. It is extremely difficult to prepare such thin BDD tubes by direct synthesis or molding from powders. To obtain thin BDD tubes, direct shaping from a BDD block is required.

The chemical vapor deposition (CVD) is currently a powerful industrial method to synthesize diamond and BDD films. Recently, we found companies that produce and deal CVD-BDD blocks with dimensions of $10\times10\times1.2$ mm^3. These dimensions allow manufacturing heaters for the smallest MAA assemblies. Therefore, it should be more practical to purchase CVD-BDD blocks from company and manufacture heaters from them than to synthesize BDD blocks by high-pressure experiments. In this study, we shaped CVD-BDD

blocks in tubular shapes by two methods, and tested their heating performance in MAA assemblages.

2. Materials and methods

A. Preparation of tubular CVD-BDD heater

The CVD-BDD blocks used in this study had dimensions of 10×10×1.2 mm^3 (Figure 1a,d), and were purchased from Changsha 3 Better Ultra-hard Materials Co., Ltd. in a price of ~65 Euro/piece. The product description of this item shows a boron content of 0.5 wt.%, which is the highest boron content of BDD commercially provided by companies to the best of our knowledge.

BDD tubes were manufactured by the following two methods.

As a heating element, BDD is electrically conductive. In the first method, manufacturing was, therefore, made by the electric discharge machining (EDM). We used a micro electric discharge machine system to manufacture BDD tubes. A tungsten rod with 0.6-mm diameter was used as an electrode for boring an inner hole of a BDD tube and a molybdenum tube with 1.5-mm outer and 0.9-mm inner diameters as an electrode for manufacturing an outer surface of the BDD tube. The discharging energy was set to be 20 μJ with a peak power of 0.8 W. The machining process took around 3 days to produce one tube.

As the black color of BDD shown, BDD is a good absorber of visible light. BDD blocks were therefore cut by a laser in the second method. The cutting was conducted by a company (Dutch Diamond Technologies BV) using a green laser with a wavelength of 532 nm. Production of 64 pieces costed around 1200 Euro.

B. Characterization of CVD-BDD

The BDD blocks and tubes were characterized by a micro-focused X-ray diffraction (XRD) and a scanning electron microscope (SEM). Figure 1(b,e) show top and side views of a BDD tube shaped by EDM. A BDD tube with dimensions of 0.9/0.6/1.2 mm was successfully fabricated. However, the surface of BDD tube was contaminated by small amounts of Mo oxide (Mo_4O_{11}) as shown by the micro-focused X-ray diffraction pattern (Figure 2). The inner wall should also be contaminated by small amounts of W oxide although we were not able to check

it by X-ray diffraction due to experimental difficulty. We also tried to remove the Mo oxide by rinsing the BDD tube in 10 wt.% HCl solution for more than 12 hours at ~100 °C. The X-ray diffraction pattern (Figure 2) and SEM images (Figure 3 (c, d)), however, show that the Mo oxide remained, which may limit high temperature generation of this heater (Table 1).

Figure 1 (c,f) show top and side views of a BDD tube with dimensions of 0.9/0.6/1.2 mm manufactured by a laser. X-ray diffraction pattern (Figure 2) and SEM images (Figure 3 (e, f)) show that the surface of the BDD tube was clean without any contamination. Furthermore, we emphasize that the laser cutting can produce a much larger number of BDD tubes than EDM. We, therefore, conclude that the laser cutting is a better way than EDM. In this study, the majority of high-pressure experiments were conducted using laser-cut BDD tubes.

C. Heating tests at high pressures

The heating tests were conducted at high pressure and temperature in a 6-axis multi-anvil apparatus installed at Bayerisches Geoinstitut, University of Bayreuth [13]. Cell assemblies were compressed to 30 GPa by using sintered-diamond cubes with a 1.5 mm truncated edge length as second-stage anvils. After reaching a target press load (1.6 MN), heating was performed by power control with voltage and current limits of 50V and 60A, respectively. Temperatures were measured by a $W_{97}Re_3$-$W_{75}Re_{25}$ thermocouple.

3. Results and discussions

A. Heating performance of EDM-shaped BDD

We first tested the EDM-shaped BDD tubular heater. Figure 4a shows a schematic view of the cell assembly. An MgO octahedron with an edge length of 5.7 mm was used as a pressure medium. The heating was terminated at ~1870 K when the heating became unstable. Some metal droplets, containing W, Re and Mo, were found along the inner side of heater in the recovered sample, which suggested melting of the thermocouple (Figure 4 (b, c)). Since the melting temperature of W/Re alloy is much higher than 1870 K, the melting should have been caused by the Mo and W oxides, which remained on the BDD tube surface after manufacturing. Therefore, EDM is not an appropriate method to prepare BDD tubes for high-temperature generation.

B. Heating performance of laser-shaped BDD

Next, we tested the laser-shaped BDD tubes. In some early runs, we found that electromotive forces (thermocouple reading) were affected by the alternating voltages of the heater, because the thermocouple contacted with the heater in the cell assembly shown in Figure 4a. To overcome this problem and ensure correctness of thermocouple reading, we designed a new assembly, as shown in Figure 5 (a,b). The thermocouple was set parallel to the heater axis and was insulated from the heater using an MgO or Al_2O_3 tube, which ensures that the thermocouple is free from heater noise. In these tests, MgO octahedrons with an edge length of 5.7 mm were used as pressure media. The edges and corners of the octahedrons were truncated. The BDD tubular heaters were 1.2 or 1.6 mm in length. The 1.6 mm BDD tube was made by connecting two 0.8 mm tubes, which were ground from 1.2 mm tubes. Mo was used as electrodes.

Figure 6 shows the power-temperature and power-resistance relationships of run M772. In the first heating, temperature was gradually increased to 2270 K at a rate of ~30 K/min, and was kept for 20 minutes. The apparent resistance of the heater first decreased from 6 to ~0.9 Ω until ~1270 K, then, almost remained constant or slightly increased (Figure 6b). This behavior was similar to that of high-pressure synthesized BDD heaters [6]. To examine reproducibility of power-temperature-resistance relations, we decreased temperature to 770 K and then increased again. The power-temperature relationships show good reproducibility among the first heating, first cooling and second heating paths. In the second heating, we attempted to generate temperature as high as possible, and succeeded in generating 2670 K. The heating was, then, terminated due to the fluctuation of heater resistance. The recovered sample showed an eutectic melting among ZrO_2, Al_2O_3 and CaO (Figure 7), which should be a cause of the heater resistance fluctuation. Therefore, CVD-BDD is useful for ultrahigh temperature generation at high pressure. Considering its commercial availability with a reasonable price, a CVD-BDD heater is more practical than a high-pressure synthesized BDD heater for wide applications.

C. Remarks for ultra-high temperature generation in small cell

Figure 8 shows power-temperature relationships with different cell assemblies. The different heater lengths have only limited effects on the heating efficiency (Table 1 and Figure 8). The cell assemblies with ZrO_2 thermal insulators have much higher heating efficiencies than

those without ones. Based on our experience, heating powers should be kept below 800 W to prevent the temperatures of the anvil's tops for electrodes from exceeding the eutectic melting point of the Co-C system (~1600 K at ambient pressure). Therefore, increase of heating efficiency is essential for ultrahigh-temperature generation.

There are two methods to increase the heating efficiency: thermal insulation and decrease of heater diameters. Since the heaters diameters were already very small (0.6 mm in inner diameter), the sample space was too limited to decrease the heater dimensions furthermore. It will also be very difficult to assemble a cell when the heater dimensions were decreased. Thermal insulation is therefore essential for ultrahigh-temperature generation in small cell assemblies. Our traditional thermal insulator CaO-stabilized ZrO_2, however, is not suitable for ultrahigh-temperature generation due to an eutectic melting among ZrO_2 and CaO. Moreover, synchrotron X-ray is needed to determine pressure in small cell assemblies due to the low reproducibility of pressure generation among different runs, which in turn requires an X-ray transparent thermal insulator. The common X-ray transparent thermal insulator is boron epoxy. However, it has been recognized many disadvantages of using boron-epoxy, such as limited pressure range (practically <10 GPa), enhancing blow-out probability, and dehydrated water from epoxy. Therefore, novel X-ray transparent thermal insulating material is desired. One candidate is a recently developed boron-MgO composite [14].

ACKNOWLEDGEMENTS

We thank T. Boffa Ballaran, K. Vlasov, L. Dubrovinsky, F. Heidelbach, S. Khandarkhaeva, A. Kurnosov, T. Meier, for their help on using the electric discharging machine. We would like to thank R. Njul, and D. Wiesner for their help on polishing sample and measuring SEM, respectively. We thank Fang Xu, Chao Wang, Hongzhan Fei, Biao Wang, Takayuki Ishii, Yingwei Fei for constructive discussions. This project has received funding from the European Research Council (ERC) under the European Union's Horizon 2020 research and innovation programme (Grant agreement No. 787 527, UltraLVP).

REFERENCES

[1] Ito, E., 2007. 2.08 Theory and practice-multianvil cells and high-pressure experimental method. Mineral physics. In: Treatise on Geophysics, vol. 2, pp. 197-230.

[2] Zerr, A., Diegeler, A., Boehler, R., 1998. Solidus of Earth's deep mantle. Science, 281(5374), 243-246.

[3] Fiquet, G., Auzende, A. L., Siebert, J., Corgne, A., Bureau, H., Ozawa, H., Garbarino, G., 2010. Melting of peridotite to 140 gigapascals. Science, 329(5998), 1516-1518.

[4] Nomura, R., Hirose, K., Uesugi, K., Ohishi, Y., Tsuchiyama, A., Miyake, A., Ueno, Y., 2014. Low core-mantle boundary temperature inferred from the solidus of pyrolite. Science, 343(6170), 522-525.

[5] Andrault, D., Bolfan-Casanova, N., Nigro, G. L., Bouhifd, M. A., Garbarino, G., Mezouar, M., 2011. Solidus and liquidus profiles of chondritic mantle: Implication for melting of the Earth across its history. Earth Planet. Sci. Lett., 304(1-2), 251-259.

[6] Xie, L., Yoneda, A., Yoshino, T., Yamazaki, D., Tsujino, N., Higo, Y., Tange, Y., Irifune, T., Shimei, T., Ito, E., 2017. Synthesis of boron-doped diamond and its application as a heating material in a multi-anvil high-pressure apparatus. Rev. Sci. Inst., 88, p.093904.

[7] Ozawa, H., Tateno, S., Xie, L., Nakajima, Y., Sakamoto, N., Kawaguchi, S.I., Yoneda, A. and Hirao, N., Boron-doped diamond as a new heating element for internal-resistive heated diamond-anvil cell. High Press. Res., 38(2), 120-135.

[8] Xie, L., Yoneda, A., Yamazaki, D., Manthilake, G., Higo, Y., Tange, Y., Guignot, N., King, A., Scheel, M. and Andrault, D., 2020. Formation of bridgmanite-enriched layer at the top lower-mantle during magma ocean solidification. Nat. Comm., 11(1), 1-10.

[9] Yamada, A., Irifune, T., Sumiya, H., Higo, Y., Inoue, T. and Funakoshi, K.I., 2008. Exploratory study of the new B-doped diamond heater at high pressure and temperature and its application to in situ XRD experiments on hydrous Mg-silicate melt. High Press. Res., 28(3), 255-264.

[10] Shatskiy, A., Yamazaki, D., Morard, G., Cooray, T., Matsuzaki, T., Higo, Y., Funakoshi, K.I., Sumiya, H., Ito, E. and Katsura, T., 2009. Boron-doped diamond heater and its application

to large-volume, high-pressure, and high-temperature experiments. Rev. Sci. Inst., 80(2), 023907.

[11] Yoneda, A., Xie, L., Tsujino, N., Ito, E., 2014. Semiconductor diamond heater in the Kawai multianvil apparatus: an innovation to generate the lower mantle geotherm. High Press. Res., 34(4), 392-403.

[12] Xie, L., Yoneda, A., Yoshino, T., Fei, H., Ito, E., 2016. Graphite–boron composite heater in a Kawai-type apparatus: the inhibitory effect of boron oxide and countermeasures. High Press. Res., 36(2), 105-120.

[13] Manthilake, G., Walte, N., Frost, D. J., 2012. A new multi-anvil press employing six independently acting 8 MN hydraulic rams. High Press. Res., 32(2), 195-207.

[14] Xie, L., Yoneda, A., Xu, F., Higo, Y., Wang, C., Tange, Y., King, A., Antonangeli, D., Morard, G., Guignot, N., 2020. Boron-MgO composite as an X-ray transparent pressure medium in the multi-anvil apparatus. Rev. Sci. Inst., 91, 043903.

TABLE 1. Summary of temperature generation at ~30 GPa using CVD-BDD heaters. The heater size is defined in the order of outer diameter, inner diameter, and length. The pressures were estimated based on a calibration curve using pressure fixed points of ZnS and GaP phase transitions and a constant thermal pressure of 2 MPa/K, which was estimated by another run using synchrotron X-ray (the results will be published elsewhere). The error of estimated pressure is ~3 GPa.

Run #	**Manufacturing**	**Heater size**	**Thermal insulator**	**sample**	**Highest Temperature /K**
M714	EDM	0.9/0.6/1.2	None	MgO+10 wt. %diamond	1870
M760	Laser cutting	0.9/0.6/1.2	ZrO_2	Al_2O_3 tube	2170
M766	laser cutting	0.9/0.6/1.2	MgO	MgO tube	1970
M772	laser cutting	0.9/0.6/1.6	ZrO_2	Al_2O_3 tube +ZrO_2 tube	2670
M773	laser cutting	0.9/0.6/1.6	ZrO_2	Al_2O_3 tube +ZrO_2 tube	2270

Figure

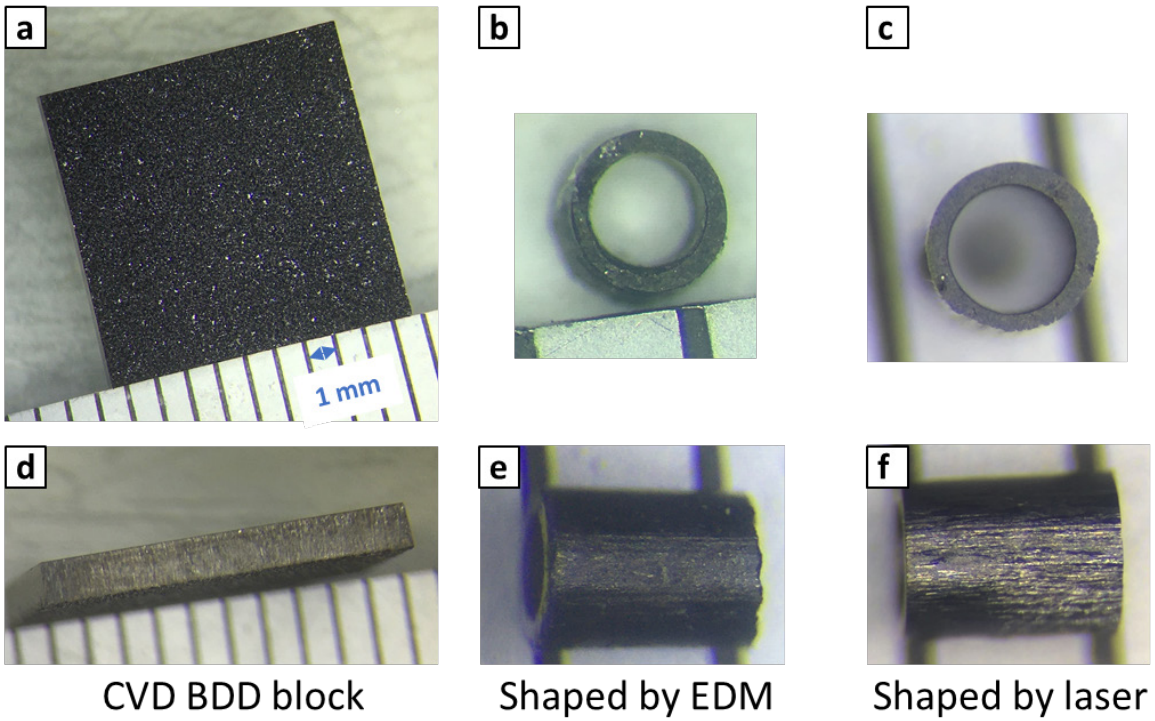

Figure 1. Microscopic images of commercial CVD-BDD blocks and manufactured tubes. (a,d) Top and side views of commercial CVD-BDD blocks, respectively. (b,e) Top and side views of a 0.9/0.6/1.2 mm BDD tube made by EDM, respectively. (c,f) Top and side views of a 0.9/0.6/1.2 mm BDD tube manufactured by laser cutting, respectively.

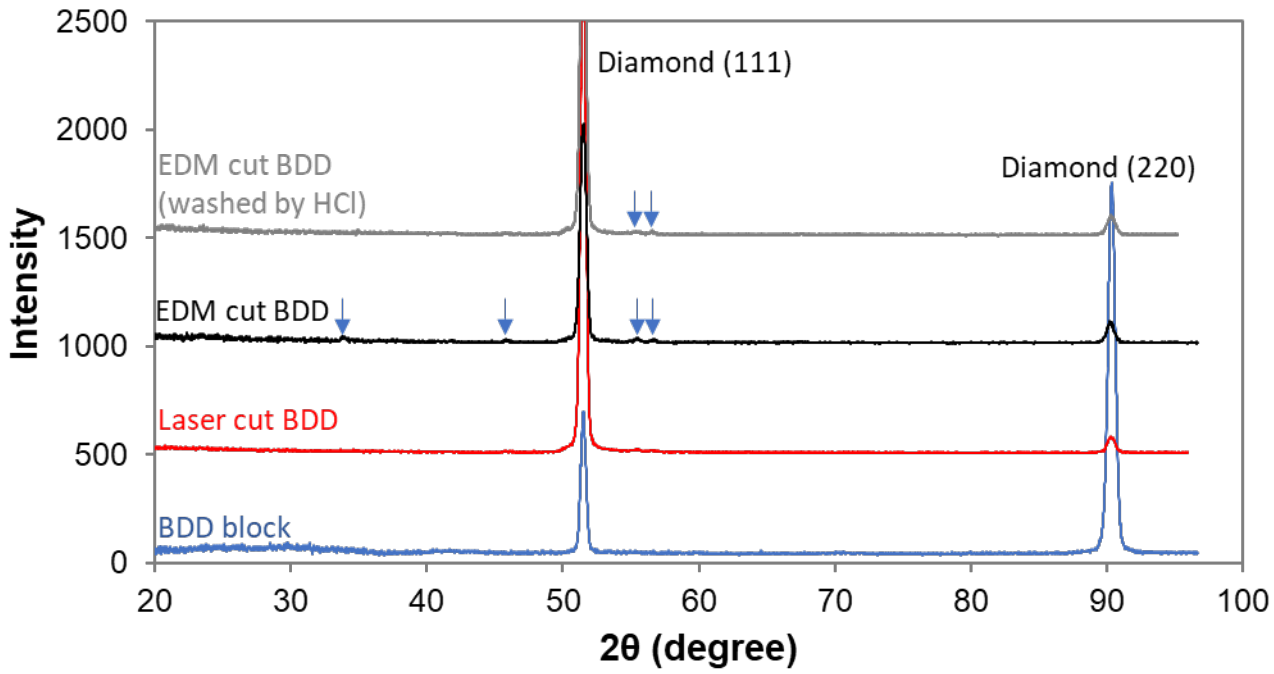

Figure 2. Micro focused X-ray diffraction patterns of a BDD block and tubes. X-ray beams with a wavelength of 1.79026 Å were focused to a 100×400 μm in diameter using an IFG polycapillary X-ray mini-lens. BDD block: the original BDD block used for cutting tubes. Laser cut BDD: BDD tube cut by laser cut method. EDM cut BDD: BDD tube cut by EDM. The HCl washed BDD tube was washed by 10 wt.% HCl for more than 12 hours. The arrows marking the small peaks, are not related to diamond or graphite. These peaks can be matched with none of Mo_2C, MoO_2, MoO_3, WC. They roughly match the peaks of Mo_4O_{11}.

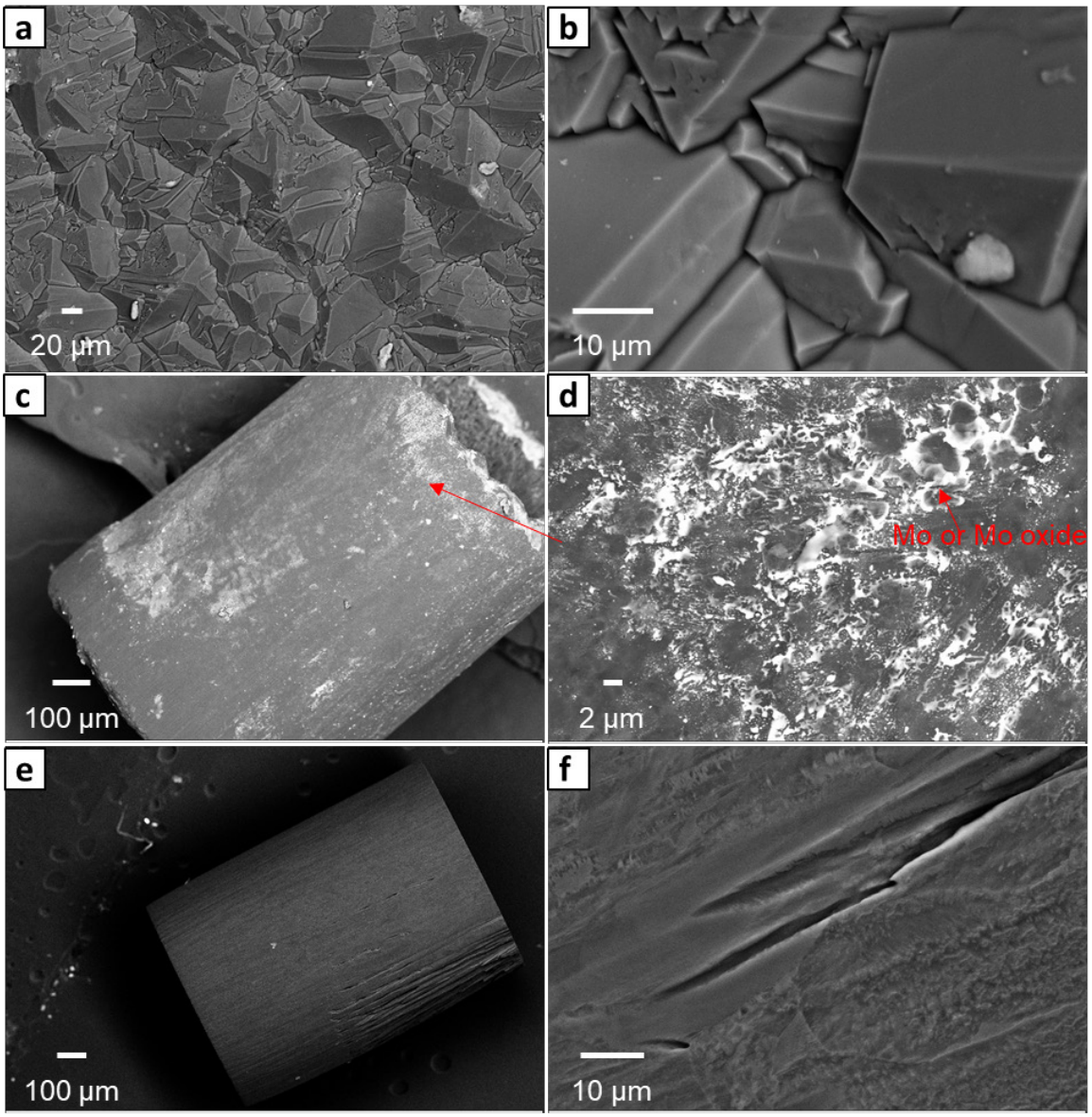

Figure 3. Backscattered electron images of the BDD block and tubes. (a,b) CVD-BDD block. (c,d) the EDM-manufactured BDD tube after washing by HCl solution. The white part on the tube is the contamination of Mo electrode. (e,f) the laser-cut BDD tube, the surface of which is clean.

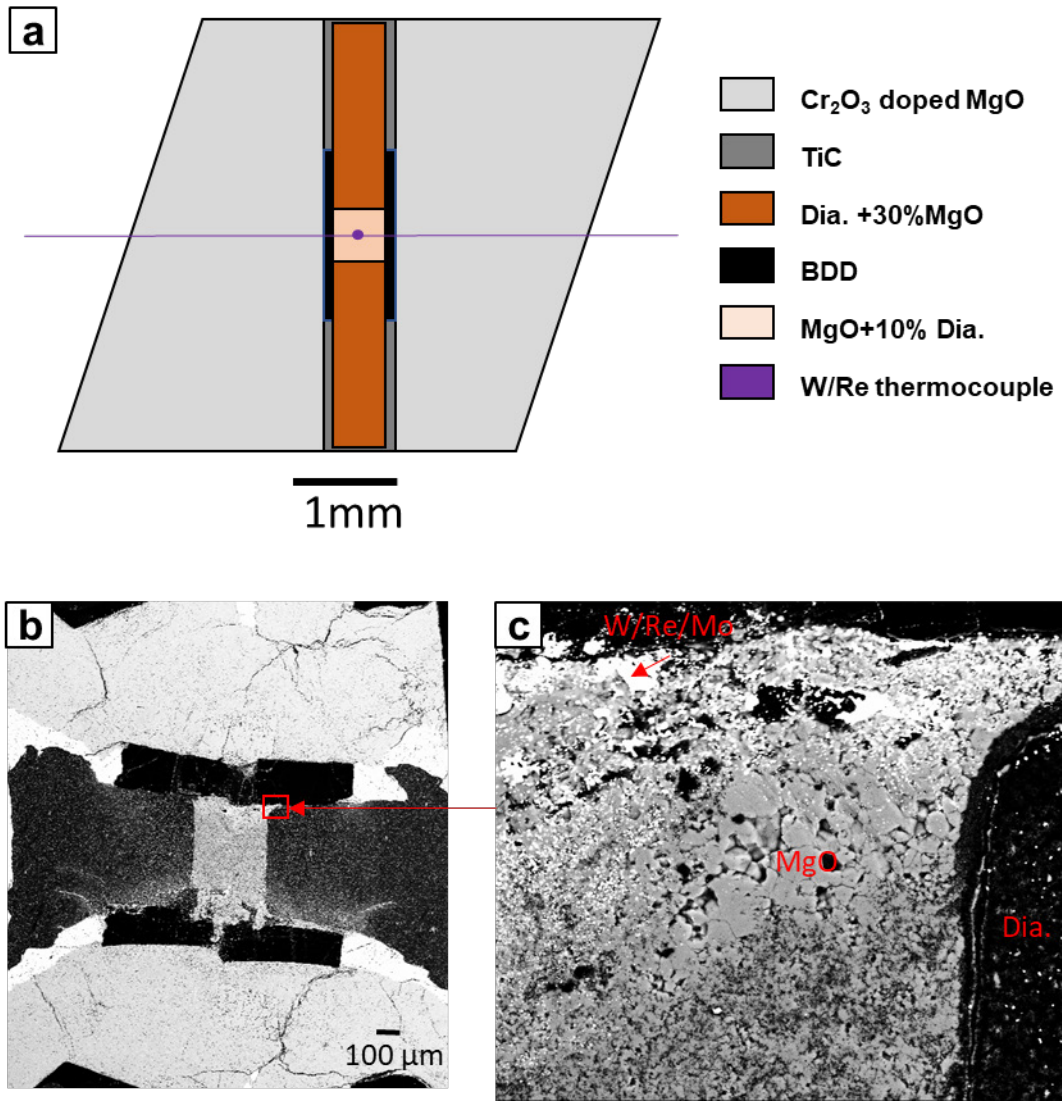

Figure 4. Experiment using the EDM-manufactured BDD tube (Run M714). (a) A schematic drawing of the cell assembly. A TiC tube was used as electrode. MgO with 10 wt% diamond (Dia.) was used as sample. (b, c) Backscattered electron images of the recovered sample. Compared with (a), the images (b) and (c) are rotated by ~90 degrees.

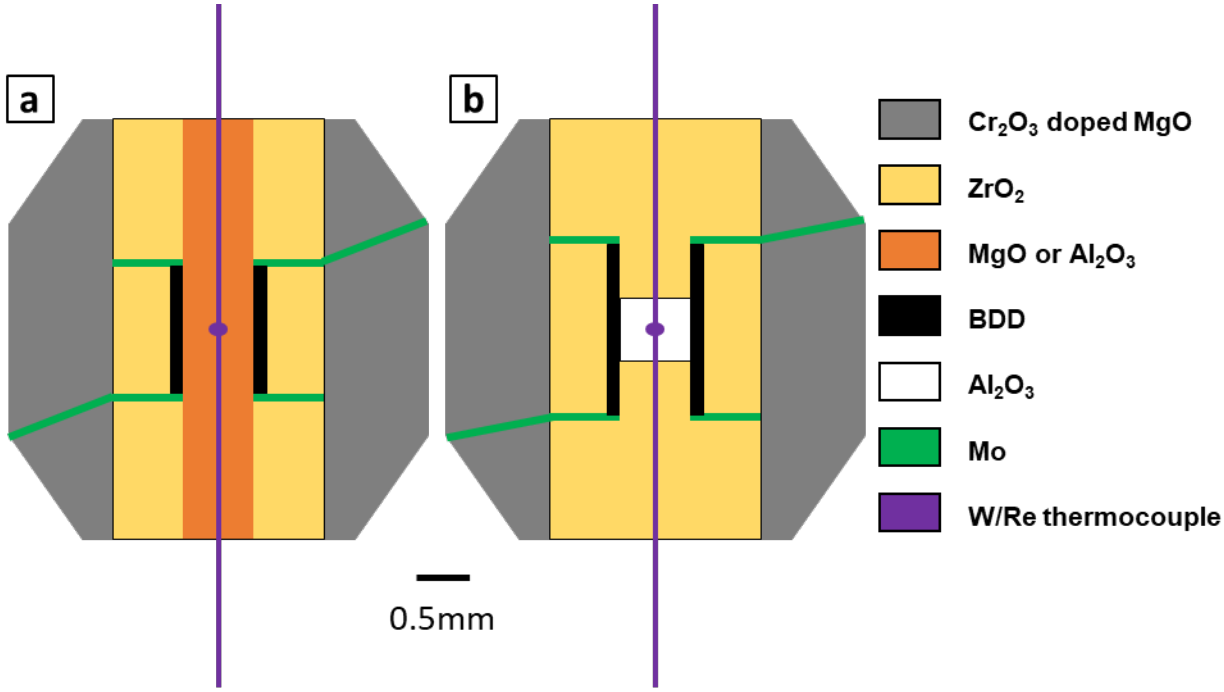

Figure 5. Cell assemblies with laser-cut BDD heaters. The heater length was 1.2 and 1.6 for assembly (a) and (b), respectively. Assembly (a) was used for M760 and M766 in Table 1; assembly (b) was used for M772 and M773 in Table 1.

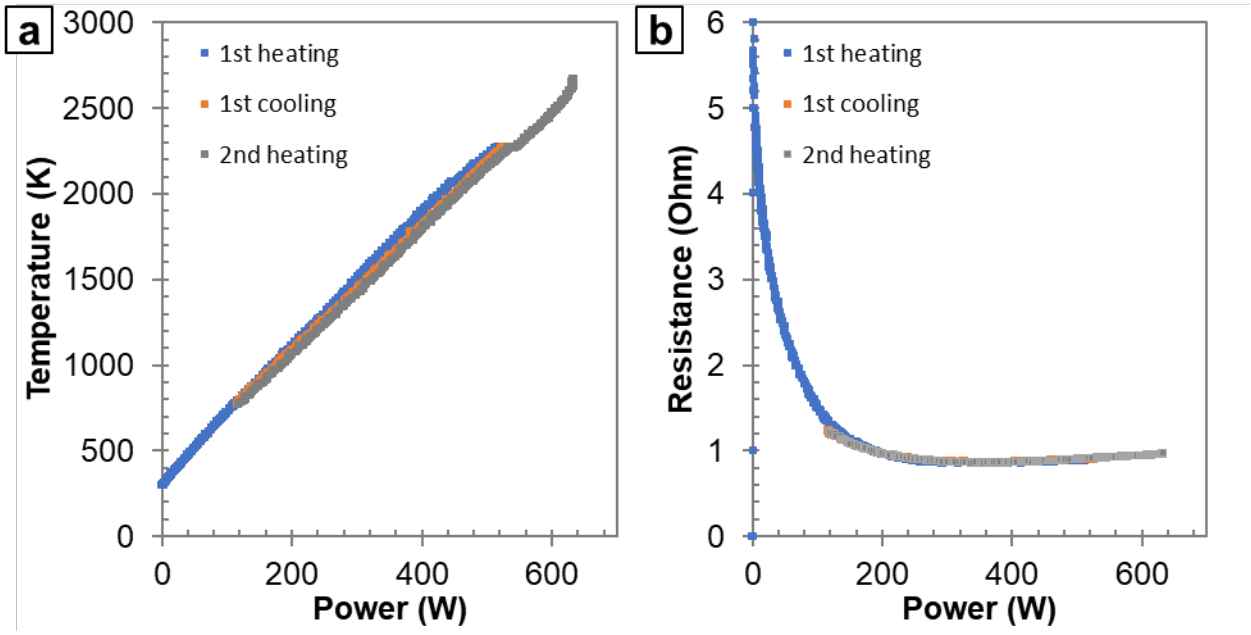

Figure 6. Power–temperature (a) and power-resistance (b) diagrams of laser-cut BDD heater (run M772).

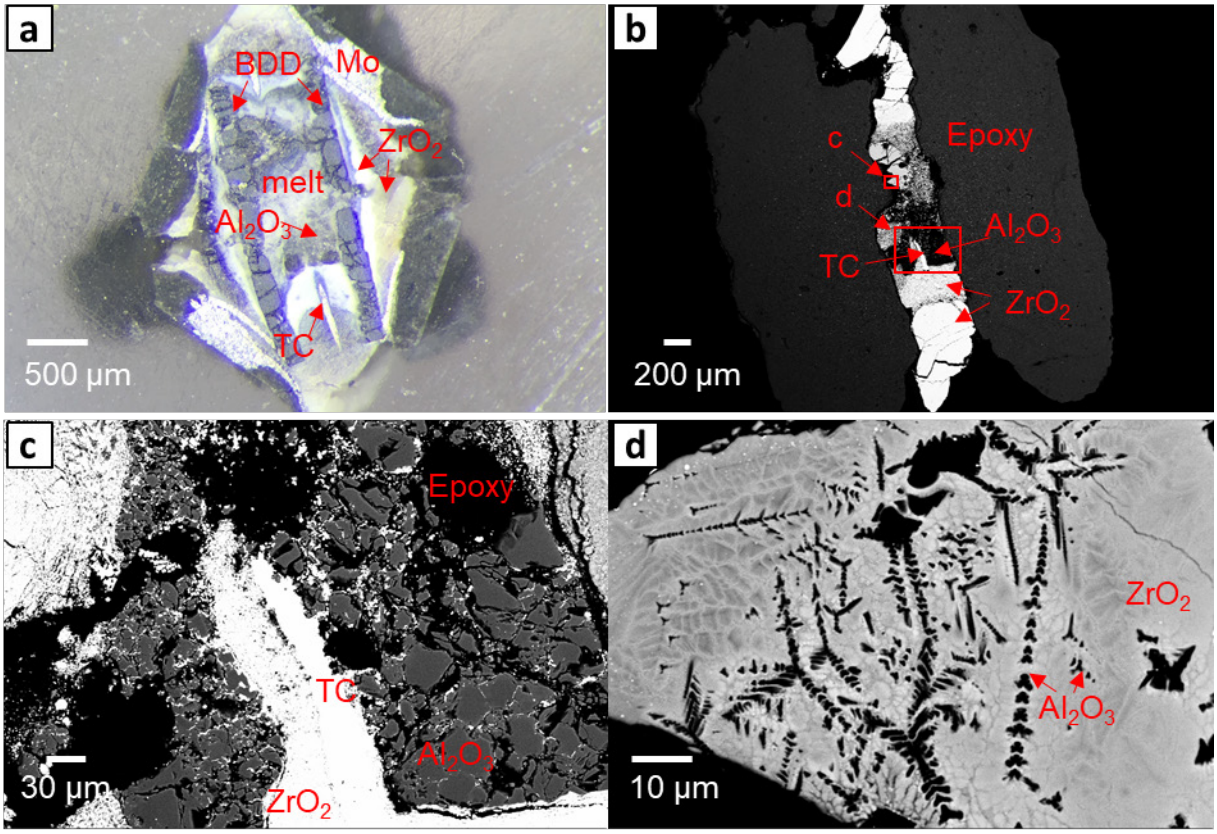

Figure 7. Optical microscopic image (a) and backscattered electron images (b, c, d) of recovered sample of run M772. (a) Optical image showing a wide view of the cell. (b) Backscattered electron image of overview of the heater inside. In order to get well polished sample, the diamond heater and cell assembly out of it was removed by diamond bits and sample was polished a ~30 μm deeper than (a). c, d rectangles mark the area of sample where image (c) and (d) were zoomed up, respectively. (c) Zoomed up backscattered electron image of rectangle c in (b). Al_2O_3 sample was not melted and grown from a grain size of ~5 μm to ~30 μm. (d) Zoomed up backscattered electron image of rectangle d in (b). Dendritic texture was found, indicating eutectic melting between sample (Al_2O_3) and thermal insulator (CaO stabilized zirconia).

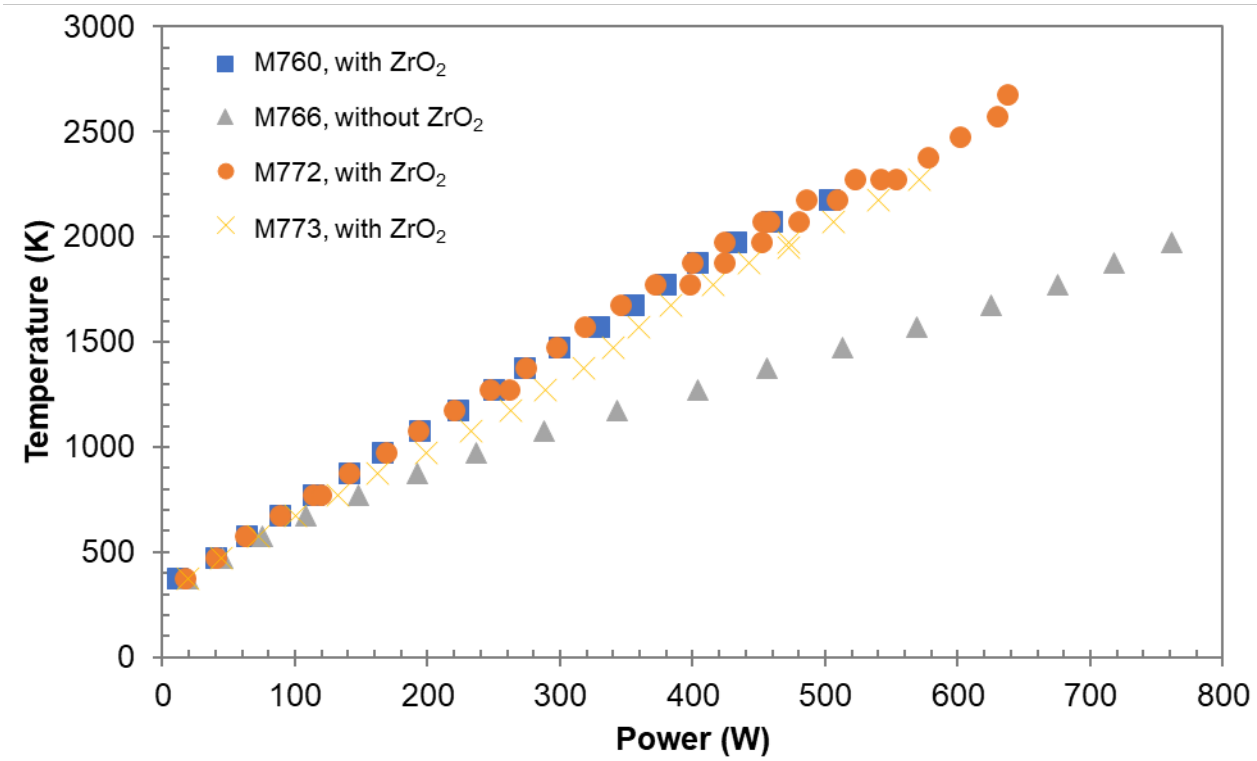

Figure 8. Summary of power–temperature relationships of laser-cut BDD heaters.